

## Pattern dynamics in a checkerboard map

N. J. Balmforth

*Departments of Mathematics and Earth and Ocean Science, University of British Columbia, Vancouver, British Columbia V6T 1Z2, Canada*

E. A. Spiegel<sup>a)</sup>

*Department of Astronomy, Columbia University, New York, New York 10027*

(Received 8 April 2004; accepted 1 July 2004; published online 16 September 2004)

Differential equations often have solutions in the forms of trains of coherent structures such as pulses and antipulses. For such systems, the methods of singular perturbation theory permit the derivation of pattern maps that predict the sequence of spacings between successive pulses. Here we apply such a procedure to cases where two distinct kinds of pulse (or antipulse) may coexist in the system. In that case, direct application of the method leads to multivalued maps that make for complicated descriptions, especially when the succession of pulse types becomes chaotic. We show how this description may be simplified by using maps arrayed in checkerboard style to provide causal descriptions of both the successions of pulse spacings and the order in which the different kinds of pulse go by. © 2004 American Institute of Physics. [DOI: 10.1063/1.1784752]

**Dissipative systems of differential equations exhibit the same kind of wave particle duality that one sees in conservative systems. Here, by particle, we mean a long-lived solitary wave that emerges as a simple nonlinear solution of the basic equations. When several of such discrete objects form, it becomes difficult to solve the nonlinear partial differential equations that spawn them. Instead, one may discretize the system by reducing it to equations of motion for the solitary structures, allowing for their interactions. This reduction is quite effective as long as the structures remain widely separated. In that case the tidal distortions are small and perturbative procedures are quite accurate. So that this approach should lead to finite results, we must impose a condition that is a standard of this kind of procedure—called singular perturbation theory—to ensure that it leads directly to finite results. However, when the system admits more than one kind of solitary wave, those results are unwieldy. Hence the aim of the present work is to describe a simplifying procedure that renders the results manageable and leads to rules that predict both the successive spacings of the solitary structures and the succession of wave types in a given train of them. To keep the presentation relatively brief, we study only the case where there exists a frame of motion in which the spacings of the structures remain constant in time, but we indicate briefly how a more general approach may be formulated.**

grounds such as dimensional arguments and, for this reason, they are called coherent structures. The earliest studies of such objects were made in the context of conservative systems as in relativity<sup>1</sup> and quantum field theory.<sup>2</sup> In those subjects, the coherent structures are likened to material particles whose dynamics may be described by equations of motion derived from the underlying field theory. Such reductions are desirable when more than one coherent structure arises, for then the objects interact and the subsequent evolution becomes difficult to analyze in the field theory. Similar approaches have been developed for the study of coherent structures in dissipative field theories, both for pulses and kinks.<sup>3–9</sup>

One reason for raising the distinction between the conservative and the dissipative field theories lies in a comparison of the corresponding kinds of dynamical system. In the conservative case, a periodic orbit will retain any energy it is assigned; in dissipative systems, the stable periodic orbits are the more rigidly prescribed limit cycles. This distinction between the two cases carries over to the spatial structures so that, in the dissipative case, the derived equations of motion tend to be more constraining.

Our discussion here concerns an aspect of the derivation of equations of motion for the coherent structures that appear in the study of dissipative nonlinear partial differential equations in one space dimension only and in time. When only one kind of coherent structure is admitted, the derivation of approximate equations of motion by asymptotic means has been thoroughly documented in the references just cited. We shall briefly sketch the general approach for this case in Sec. IB as a prelude to a discussion of the feature of this problem that is of particular interest to us in this study. Accordingly, we consider situations in which two different kinds of coherent structure enter the dynamics. We confine attention here to the simplest case in which there exists a reference frame in which the resulting pulse train is steady. The pattern theory that then arises involves multivalued maps and our aim is to

### I. INTRODUCTION

#### A. Statement of the problem

Many nonlinear field theories yield solutions in the form of localized structures or solitary waves. These typically exist for longer times than might be anticipated on naive

<sup>a)</sup>Electronic mail: eas@astro.columbia.edu

show how to rearrange these results into checkerboards of maps of the interval.<sup>10</sup> These are single-valued maps of a composite interval that carry information on the nature of the successive pulses as well as on their spacing.

**B. Sketch of the method**

Let  $\mathbf{u}(x, t)$  be a set of scalar fields in a two-dimensional space-time  $(x, t)$ . Suppose that we are given field equations in the form

$$\partial_t \mathbf{u} = \mathcal{L}_{\mathbf{p}}(\partial_x) \mathbf{u} + \mathcal{N}(\mathbf{u}). \tag{1.1}$$

Here  $\mathcal{L}_{\mathbf{p}}$  is a linear differential operator that depends on parameters  $\mathbf{p}$  and  $\mathcal{N}$  is a strictly nonlinear operator that may similarly contain spatial derivatives and parameters. We assume that  $|\mathbf{u}|$  goes rapidly to zero as  $|x|$  goes to  $\pm\infty$ . There is no explicit time dependence in either operator.

We first assume the existence of a solitary solution of the equation that is steady in a frame moving in  $x$  at speed  $c$ . Such a solution has the form

$$\mathbf{u}(x, t) = \mathbf{U}(\chi) \quad \text{for} \quad \chi = x - ct. \tag{1.2}$$

When we introduce Eq. (1.2) into Eq. (1.1), we obtain the ordinary differential equation

$$\mathcal{L}_{\mathbf{p}}(D) \mathbf{U} + cD \mathbf{U} + \mathcal{N}(\mathbf{U}) = 0. \tag{1.3}$$

In the far wings of the solitary structure,  $|\mathbf{U}|$  is quite small and we may linearize the equation in those regions; that is, we linearize about the state  $\mathbf{U} = \mathbf{0}$ . The equation is constructed so that linearization is achieved by dropping the term  $\mathcal{N}(\mathbf{U})$ . The linearized equation admits solutions whose  $\chi$ -dependence is like  $\exp[(\sigma + i\omega)\chi]$ . We consider only the simple case where for suitable parameter values there are just two eigenvalues (if we count a complex conjugate pair as a single eigenvalue) with the property that one of the roots (or pairs) has positive real part and the other has negative real part. Thus one solution decays in the positive  $\chi$  direction and the other in the negative  $\chi$  direction. Then we may further seek conditions in which the two linear solutions form the wings of one or more types of pulsatile solutions, when we regard  $\chi$  as analogous to time in a dynamical system. There is a great range of possible types of such homoclinic solutions distinguished in particular by the number of times they wind around the various fixed points of the system. We shall work with only a very few of the simplest forms of these and merely cite two attempts to classify some of the possibilities.<sup>11,12</sup>

Finding a homoclinic solution involves a determination of the parameters for which it may exist. If we specify parameter values  $\mathbf{p}_0$ , we need then to find the values of  $c(\mathbf{p}_0)$  for which one or, as in the following, more such solutions exist. The simplest and most studied situation is the one in which, for given  $\mathbf{p}_0$ , there is only one homoclinic solution (or pulse)  $\mathbf{U} = \mathbf{H}(\chi)$  with its maximum value placed arbitrarily at  $\chi = 0$ . When  $\varepsilon = |\mathbf{p} - \mathbf{p}_0|$  is sufficiently small, numerical solutions to the problem typically take the form of a series of widely separated, propagating pulses. Then we may look for approximate solutions in the form of series of pulses whose separations become larger as  $\varepsilon$  gets smaller. This form of solution may be written (in the case of  $N$  pulses) as

$$\mathbf{u}(x, t) = \sum_{k=1}^N \mathbf{H}(\chi - \chi_k) + \varepsilon \mathcal{R}(\chi, \{\chi_k\}, \varepsilon), \tag{1.4}$$

where  $\varepsilon \mathcal{R}$  is the error made in assuming that a linear superposition of coherent structures approximates a nonlinear solution.

As part of the approximation, we let  $\mathcal{R}$  depend on  $\chi$  and on the set of instantaneous positions  $\{\chi_k\}$  at which the pulses are found in the moving frame. The idea is then to keep the error small by requiring  $\mathbf{R}$  to be finite through a solvability condition arising in the asymptotic development. This condition fixes the  $\chi_k$  in the special case where the spacings are stationary in some appropriate frame. The situation is then the same if the original problem is posed as an ordinary differential equation and  $\chi$  is actually the time. Then the same sort of approximation may be introduced and the development based on Eq. (1.4) leads to maps of the pulse spacings equivalent to those found using the arguments of Shilnikov.<sup>12,13</sup> However, for partial differential equations, the initial conditions will typically involve a set of  $\chi_k$  that do not accord with the results of this map. To deal with this feature of the solutions, we may let  $\chi_k$  be a function of  $\varepsilon t$ . Then the solvability condition leads instead to equations of motion for the pulses, seen as particles. These equations typically allow the pulses to relax into fixed spacing (in a suitable frame) that do accord with the spacing map, though we have no proof that this relaxation always takes place.

When more than one kind of pulse enters the dynamics, we may seek equations of motion for them. In our experience, pulse trains tend to lock into fixed spacings. So, to keep our discussion of this more complicated case as simple as possible, we assume that the pulse train has already locked into a solution that is steady in the appropriate moving frame. Thus we are really treating only the ODE (1.3). The maps for this steady case generally are multivalued, as it will turn out, and we describe how to deal with this inconvenience by introducing arrays of interval maps that have been called checkerboard maps.<sup>10</sup> A clue to the way to do this comes from the case where a pulse and its mirror image enter the problem.<sup>12,14</sup> We shall proceed in an illustrative example that we describe next.

**C. The example**

To illustrate the problem of multiple pulse types, we turn to the general equation for the dynamics of waves in thin films.<sup>15-17</sup> This is an asymptotic description of two-dimensional flow in a thin liquid film with horizontal velocity  $u(x, t)$  given by

$$\partial_t u + u \partial_x u + \kappa u^2 \partial_x u = \xi \partial_x^2 u + \eta \partial_x^3 u + \zeta \partial_x^4 u, \tag{1.5}$$

where  $\xi, \eta, \zeta$ , and  $\kappa$  are constants. When we look for solutions in the form (1.2), we are led to the ordinary differential equation

$$\frac{d^3 U}{d\chi^3} + \mu \frac{d^2 U}{d\chi^2} + \frac{dU}{d\chi} - \beta U + \alpha U^2 + U^3 = 0, \tag{1.6}$$

where the variables have been scaled so that there are only three control parameters,  $\alpha, \beta$ , and  $\mu$ , as indicated. This

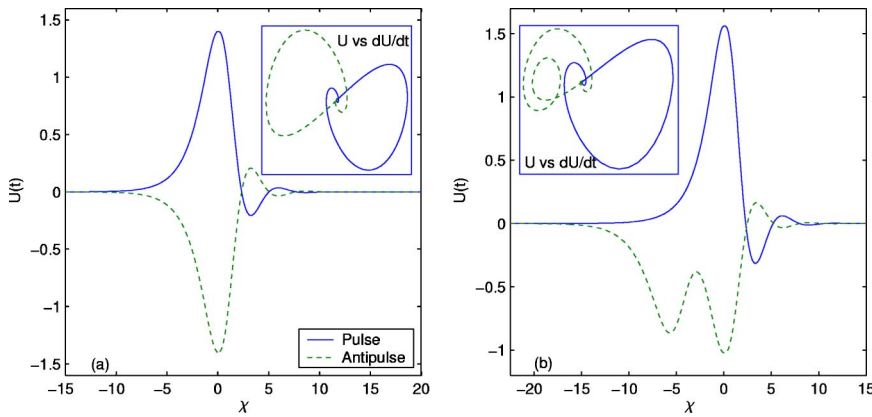


FIG. 1. (Color online) Pulse and anti-pulse solutions to Eq. (1.3). Inset panels show phase portraits projected onto the  $(U, \dot{U})$  plane. Panel (a) shows a case with symmetry ( $\alpha=0, \mu=0.7, \beta=1.107887$ ). Panel (b) shows a case in which the pulse has a single primary peak, but the anti-pulse has two peaks ( $\alpha=-3.672, \mu=0.81645, \beta=0.852806$ ).

ODE is a particular case of a model equation from the study of convection with competing instabilities.<sup>18,19</sup> The examples with either the ultimate or the penultimate term on the left omitted have been studied in some detail.<sup>19-21</sup> Partial differential equations whose traveling waves are described by an ODE of the same genre arise in several disciplines.<sup>22-24</sup> As we already mentioned, we may think of Eq. (1.6) as a dynamical system with  $\chi$  playing a role analogous to time. We shall study choices of the parameters where the solutions of Eq. (1.6) are trains of widely separated solitary structures that may be of different types.

**II. EXPANSIONS IN PULSES**

**A. Homoclinic orbits**

Equation (1.6) has three fixed points when  $\chi$  is considered as a time:

$$U=0, \quad U=U_{\pm}=\frac{1}{2}(\pm\sqrt{\alpha^2+4\beta}-\alpha). \tag{2.1}$$

Each of these organizes the flow in particular regions of the phase space  $(\dot{U}, U)$ , but we concentrate on parameter regimes in which the dominant features of the solutions are homoclinic orbits issuing from the origin. These are the orbits that asymptote to the origin as  $\chi \rightarrow \pm\infty$ . Even this restricted class of orbits has many variants, but we shall be concerned with only those orbits that, having emerged from the origin, then encircle one of the other fixed points  $U_{\pm}$  only once or twice before returning back to the origin. The orbits looping around the positive fixed point  $U_+$  have predominantly positive amplitude, and we refer to them as pulses; those that encircle  $U_-$  and traverse mainly the region  $U < 0$  of phase space are the anti-pulses; examples are shown in Fig. 1.

Such coherent structures can be found when the parameter values lie in certain surfaces in parameter space given by a condition of the form

$$\mu = \mu(\alpha, \beta). \tag{2.2}$$

These conditions define what we call the *homoclinic loci*.<sup>12</sup>

**B. The expansion**

For parameter values very near to a homoclinic locus given by Eq. (2.2), there are solutions that take the form of trains of widely spaced pulses, as one sees with a little nu-

merical exploration. Since we are interested in deriving approximate solutions containing a mixture of pulses and anti-pulses, we choose the value of  $\mu$  to bring us close to values  $\alpha = \alpha_0$  and  $\beta = \beta_0$  for which a pulse and anti-pulse coexist. Then we develop around this special condition using the small parameter  $\varepsilon$  and write

$$\alpha = \alpha_0 + \varepsilon \alpha_1, \quad \beta = \beta_0 + \varepsilon \beta_1. \tag{2.3}$$

For the development to be meaningful, we need to assume that the amplitudes of the overlapping portions of individual structures are  $O(\varepsilon)$ . If their separations are much smaller than this condition allows, we cannot reliably distinguish the pulses. For extremely large separations, we basically see isolated structures. Moreover, a large enough separation leaves open regions that may be unstable to the formation of new pulses; this raises an issue that needs special treatment.<sup>25</sup>

As a measure of the size of the typical pulse separation,  $L$ , we choose

$$\varepsilon = e^{-L\sigma}, \tag{2.4}$$

where  $\sigma^{-1}$  is a characteristic decay length fore and aft. With  $\varepsilon$  as the small parameter (or  $L$  a large one), we take the other parameters,  $(\mu, \alpha_1, \text{ and } \beta_1)$  to be of order unity.

With  $\varepsilon$  small, we are in the nearly homoclinic conditions that obtain close to  $(\alpha_0, \beta_0)$ . We designate a single homoclinic structure as  $H(\chi; \vartheta)$ , where the phase of  $\chi$  is chosen so that the extreme is at zero argument and the parameter  $\vartheta$  identifies the nature of the pulse, as explained in the following. In a series of  $N$  pulses, we approximate the  $k$ th one as  $H_k = H(\chi - \chi_k; \vartheta_k)$  where the sequence of pulses is ordered so that  $\chi_{k+1} > \chi_k$ .

The slight generalization of Eq. (1.4) for more than one kind of solitary structure that we need as an approximate solution to Eq. (1.3) is

$$u = \sum_{k=1}^N H_k + \varepsilon \mathcal{R}(\chi, \{\chi_m\}, \{\vartheta_k\}, \varepsilon), \tag{2.5}$$

where  $\varepsilon \mathcal{R}$  is the error made in assuming a solution in the form of a linear superposition. Near the core of a particular pulse, the error in its neighborhood comes mainly from the tails of the nearest neighbors and this has been tuned to be  $O(\varepsilon)$ . When we insert this ansatz into Eq. (1.3) we recover in leading order the fact that a single pulse is a solution of the basic equation. Thus

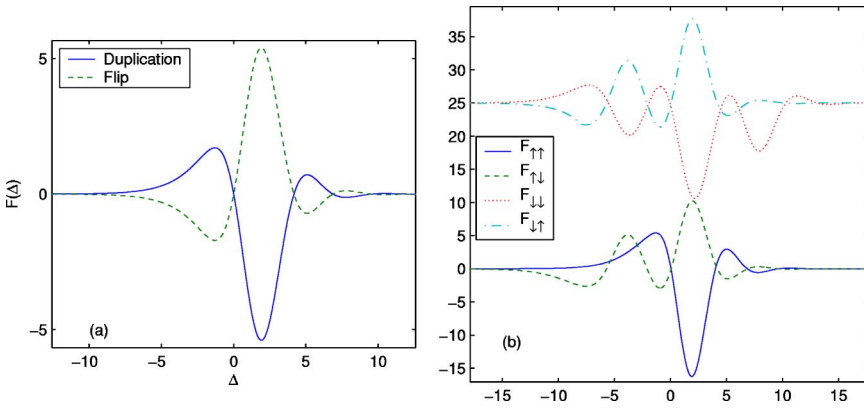


FIG. 2. (Color online) Spacing functions,  $F_{jk}(\Delta)$ , corresponding to the homoclinic orbits shown in Fig. 1. In (a), the pulse and antipulse are mirror images and  $F_{\uparrow\uparrow}(\Delta) = F_{\downarrow\downarrow}(\Delta) \equiv F(\Delta) \equiv -F_{\uparrow\downarrow}(\Delta) = -F_{\downarrow\uparrow}(\Delta)$ . The “duplication” function is  $F(\Delta)$ ; the “flip” function is  $-F(\Delta)$ . In (b), there is no such symmetry; the functions  $F_{\uparrow\uparrow}$  and  $F_{\downarrow\downarrow}$  are offset for clarity.

$$\left( \frac{d^3}{d\chi^2} + \mu \frac{d^2}{d\chi^2} + \frac{d}{d\chi} - \beta_0 \right) H_k + H_k^3 + \alpha_0 H_k^2 = 0. \quad (2.6)$$

The nearest neighbors to this pulse are each  $O(\varepsilon)$  in amplitude for  $\chi$  near  $\chi_k$  while those beyond are even smaller in that neighborhood. Hence the interaction between nearest neighbors is strongest and it enters at order  $\varepsilon$ . The terms of order  $\varepsilon$  give

$$\mathcal{L}_k \mathcal{R} = \beta_1 H_k + \alpha_1 H_k^2 - \frac{1}{\varepsilon} f(H_k) [H_{k+1} + H_{k-1}], \quad (2.7)$$

where

$$\mathcal{L}_k = \left( \frac{d^3}{d\chi^2} + \mu \frac{d^2}{d\chi^2} + \frac{d}{d\chi} - \beta_0 \right) + f(H_k), \quad (2.8a)$$

and

$$f(H) = 3H^2 + 2\alpha_0 H^2. \quad (2.8b)$$

Since  $H_{k\pm 1}$  is  $O(\varepsilon)$  near  $\chi_k$ , the last term on the right of Eq. (2.7) is  $O(1)$ .

To ensure that the error term in Eq. (2.5) is  $O(\varepsilon)$ , we require that  $\mathcal{R}$  be finite. We therefore impose the condition that the solution of Eq. (2.7) should be soluble in finite terms. For this, the inhomogeneous term on the right of Eq. (2.7) must be orthogonal to the null vector of  $\mathcal{L}_k^\dagger$ , the adjoint of  $\mathcal{L}_k$ . To define the adjoint, we adopt integration in  $\chi$  from  $-\infty$  to  $+\infty$  as the inner product in the space of functions which vanish for  $\chi \rightarrow \pm\infty$ . We find that the adjoint operator is

$$\mathcal{L}_k^\dagger = \left( -\frac{d^3}{d\chi^3} + \mu \frac{d^2}{d\chi^2} - \frac{d}{d\chi} - \beta_0 \right) + f(H_k). \quad (2.9)$$

The existence of null vectors,  $N_k = N(\chi - \chi_k, \vartheta_k)$ , of the adjoint operator has been demonstrated by L. N. Howard (personal communication) and they are not hard to compute numerically. Then, the condition that the right-hand side of Eq. (2.7) should be orthogonal to these null vectors is

$$\begin{aligned} & \beta_1 \int_{-\infty}^{\infty} N_k H_k d\chi - \alpha_1 \int_{-\infty}^{\infty} N_k H_k^2 d\chi \\ &= \frac{1}{\varepsilon} \int_{-\infty}^{\infty} N_k f(H_k) [H_{k+1} + H_{k-1}] d\chi. \end{aligned} \quad (2.10)$$

This condition controls the spacings of the sequence of pulses and it is a generalization of previous versions in which all the pulses are alike or are mirror images of each other.<sup>12,14</sup>

We let  $\Delta_k = \chi_k - \chi_{k-1}$  and write  $H_{k+1} = H(\chi - \chi_k + \Delta_{k+1}, \vartheta_{k+1})$ . If we define the function  $F_{k,j}(\Delta)$  by the relation

$$F_{k,j}(\Delta) = \frac{1}{\varepsilon I_k} \int_{-\infty}^{\infty} N_k(\chi) f[H_k(\chi)] H_j(\chi + \Delta) d\chi, \quad (2.11)$$

where

$$I_k = \int_{-\infty}^{\infty} N_k(\chi) H_k(\chi) d\chi, \quad (2.12)$$

Eq. (2.10) becomes the return map,

$$\beta_1 - S_k = F_{k,k+1}(-\Delta_{k+1}) + F_{k,k-1}(\Delta_k), \quad (2.13)$$

with

$$S_k = \frac{\alpha_1}{\varepsilon I_k} \int_{-\infty}^{\infty} N_k(\chi) H_k^2(\chi) d\chi. \quad (2.14)$$

Sample spacing functions,  $F_{jk}(\Delta)$ , are shown in Fig. 2. The functions possess structure near the core of the pulse, but decay exponentially to the right and left; in the examples shown, the functions decay with oscillations to the right.

### C. Spacing and polarity maps

Condition (2.13) determines the spacing,  $\Delta_{k+1}$ , given  $\Delta_k$  and the polarities of the previous two pulses. In fact, the relation gives more than this since it also determines the polarity of  $(k+1)$ st pulse, as we shall illustrate once we have introduced some notation.

To represent polarity, we set  $\vartheta_k = 1$  if the  $k$ th object is a pulse, and  $\vartheta_k = -1$  if it is an antipulse. The dependencies of the function  $F_{j,k}$  are then written more transparently as

$$F_{j,k}(\Delta) = F(\Delta; \vartheta_k, \vartheta_j), \quad (2.15)$$

and the spacing map as

$$C_1(\vartheta_k) = F(-\Delta_{k+1}; \vartheta_k, \vartheta_{k+1}) + F(\Delta_k; \vartheta_k, \vartheta_{k-1}), \quad (2.16)$$

where

$$C_1(\vartheta_k) = \beta_1 - S(\vartheta_k). \tag{2.17}$$

To streamline the formulas even further in considering specifically pulses or antipulses, we replace the  $\vartheta_k$  arguments with the subscripts,  $\uparrow$  and  $\downarrow$ , for  $\vartheta = \pm 1$ .

Our task is now to make sense of Eq. (2.16), which is to be solved for  $\Delta_{k+1}$  and  $\vartheta_{k+1}$ , knowing  $\Delta_k$ ,  $\vartheta_{k-1}$ , and  $\vartheta_k$  from the previous pair. If a pulse train begins with a succession of *pulses*, then the spacing map is simply

$$F_{\uparrow\uparrow}(-\Delta_{k+1}) = C_{1,\uparrow} - F_{\uparrow\uparrow}(\Delta_k). \tag{2.18}$$

As long as one can invert  $F_{\uparrow\uparrow}(-\Delta_{k+1})$ , the pulse train continues indefinitely. However,  $F_{\uparrow\uparrow}(-\Delta_{k+1})$  can be inverted only when  $C_{1,\uparrow} - F_{\uparrow\uparrow}(\Delta_k)$  is positive since  $F_{\uparrow\uparrow}(\Delta)$  returns a positive value for sufficiently large and negative argument (see Fig. 2). Consequently, when  $C_{1,\uparrow} - F_{\uparrow\uparrow}(\Delta_k)$  becomes negative (and this does happen), the continuation fails. This noninvertibility does not signal a breakdown of the asymptotic theory. It is simply what happens at a switch of polarity when the trajectory in phase space finds its way around the stable manifold into the origin and enters the region where  $U < 0$ . Then the trajectory follows a path close to the homoclinic orbit lying chiefly in  $U < 0$  to create an antipulse. Thus, a terminating iteration of Eq. (2.18) indicates a polarity reversal and the subsequent map is

$$F_{\uparrow\downarrow}(-\Delta_{k+2}) = C_{1,\uparrow} - F_{\uparrow\downarrow}(\Delta_{k+1}). \tag{2.19}$$

Since  $F_{\uparrow\downarrow}$  has negative amplitude, Eq. (2.19) can be inverted for  $\Delta_{k+2}$  when the pulses are well spaced (see Fig. 2).

Immediately after this reversal, the polarity either flips again, signifying a return to a pulse, or remains negative and antipulse follows antipulse. Those transitions are described by the conditions,

$$\left. \begin{array}{l} F_{\downarrow\uparrow}(-\Delta_{k+3}) \\ \text{or} \\ F_{\downarrow\downarrow}(-\Delta_{k+3}) \end{array} \right\} = C_{1,\downarrow} - F_{\downarrow\uparrow}(\Delta_{k+2}), \tag{2.20}$$

respectively. Which of these options one takes is determined by the sign of the right-hand side.

In summary, we iterate Eq. (2.16) by choosing the polarity of the  $(k+1)$ st pulse according to the sign of the discriminant  $C_1(\vartheta_k) - F(\Delta_k; \vartheta_k, \vartheta_{k-1})$ , and then determining the next spacing by inverting the (now invertible) function  $F_{k,k+1}(-\Delta_{k+1})$ . In the case where the train consists entirely of pulses, this procedure would be the same as has been used when only one kind of solitary object enters the dynamics and it would lead to a one-dimensional spacing map. For the more complicated problem we face here, we try to use the same kind of approach by using sequences of such simple maps. However, since there are four possible realizations of  $C_1(\vartheta_k) - F(\Delta_k; \vartheta_k, \vartheta_{k-1})$ , there are four branches of the map. The transition rules between the branches are dictated by the polarities of the current pair of pulses. We shall illustrate this complicated structure in the following, though a quick peek at Fig. 4 at this point might suggest the kind of structure we are describing.

### III. EXAMPLES

#### A. The antisymmetric case

For the antisymmetric case,  $\alpha = 0$ , pulses and antipulses are mirror images and are identical up to a sign—the polarity,  $\vartheta_k$  [see Fig. 1(a)]. This sign factors out of the various integrals in the spacing functions; also  $S_k = 0$ . The solvability condition (2.13) can be written as<sup>12,14</sup>

$$\beta_1 = \Theta_{k+1}F(-\Delta_{k+1}) + \Theta_kF(\Delta_k), \tag{3.1}$$

where  $\Theta_k = \vartheta_k\vartheta_{k-1}$  is a relative-polarity parameter, and  $F(\Delta)$  is simply  $|F(\Delta, \vartheta_j, \vartheta_k)|$  [see Fig. 2(a)]. Because  $\Theta_k$  takes either sign, we get a two-branched map of the interval,  $\Delta$ , examples of which are given in Ref. 13. With

$$\mathcal{Z}_k = F(-\Delta_k), \tag{3.2}$$

the map becomes

$$\Theta_{k+1}\mathcal{Z}_{k+1} = \beta_1 - \Theta_k\mathcal{F}(\mathcal{Z}_k), \tag{3.3}$$

where  $\mathcal{F}(\mathcal{Z}) = F[-F^{-1}(\mathcal{Z})]$ . The duplicity of the map is removed by expressing the spacing relations as a continuous map in the  $\Theta_k\mathcal{Z}_k - \Theta_{k+1}\mathcal{Z}_{k+1}$  plane. The signs of  $\Theta_k$  can then be absorbed into the definition of  $\mathcal{Z}_k$ , and the map becomes

$$\mathcal{Z}_{k+1} = \begin{cases} \beta_1 - \mathcal{F}(\mathcal{Z}_k) & \text{in } \mathcal{Z}_k > 0 \\ \beta_1 + \mathcal{F}(\mathcal{Z}_k) & \text{in } \mathcal{Z}_k < 0. \end{cases} \tag{3.4}$$

To this order in the development in  $\varepsilon$ , this map is single-valued. Second-order corrections to the map in the asymptotic theory do introduce multivaluedness at order  $\varepsilon$  through the entry of next-nearest neighbors into the interactions. Yet higher-order corrections introduce even more multivaluedness, in keeping with the expected underlying Cantorial structure.<sup>12</sup>

#### B. Weak asymmetry

We next weakly break the symmetry between the pulses and antipulses by reintroducing the term  $\alpha U$ ,<sup>2</sup> but with  $\alpha = \varepsilon$ . In the numerical example illustrated in Fig. 3, the first panel shows  $U(\chi)$ , and the second panel shows a phase portrait projected onto the  $(U, \dot{U})$  plane. The sequence of pulse spacings and polarities extracted from a much longer time series is shown against  $k$  in the third and fourth panels.

At leading order, the homoclinic solutions are again symmetrical. That is, an antipulse solution is  $-H(\chi - \chi_k) + O(\varepsilon)$  so that the structural differences between pulse and antipulse are delayed to order  $\varepsilon$  and enter only into  $\mathcal{R}$ . Hence, just as in Eq. (3.1) of the antisymmetric case, we have that

$$F(\Delta, \vartheta_j, \vartheta_k) = \vartheta_j\vartheta_kF(\Delta). \tag{3.5}$$

If we proceed as described in the discussion following Eq. (2.20), we are led to the four-branched map of the pulse spacings,  $\Delta_k$ , shown in Fig. 4. This picture compares spacings extracted from the solution of Fig. 3 with the predictions of Eq. (2.13), using the spacing functions illustrated in Fig. 2. As a test of accuracy of the asymptotics it is useful, but such a map is too unwieldy and we must simplify things.

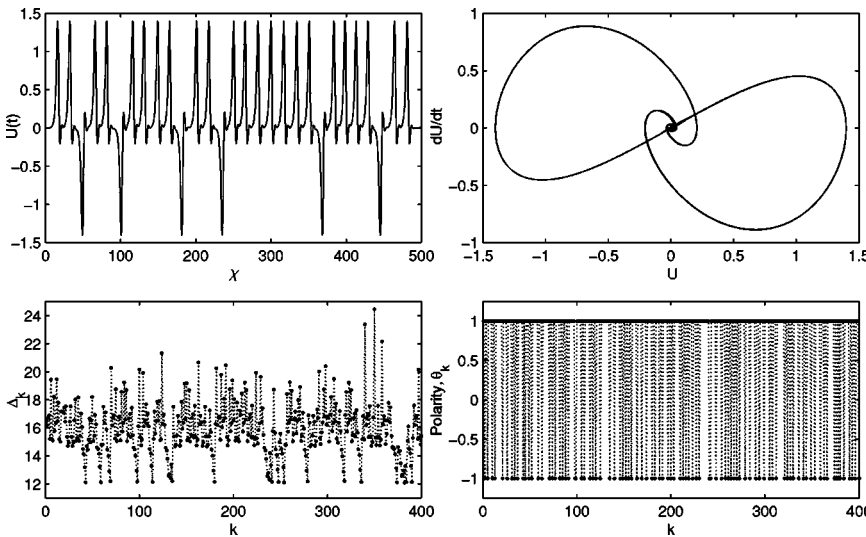


FIG. 3. A numerical solution of Eq. (1.3) with  $\mu=0.7$ ,  $\alpha=0.01$ , and  $\beta=1.108$ . The first panel shows a time series of  $U(t)$ . The second panels show a phase portrait projected on to the  $(U, \dot{U})$  plane. The solution is barely distinguishable from the nearby homoclinic orbits, and consequently the portrait looks little different from the inset of Fig. 1(a). A sequence of pulse spacings ( $\Delta_k$ ) and polarities ( $\vartheta_k$ ) taken from a much longer time series is shown in the third and fourth panels (as points connected by dotted lines).

Again, we introduce  $\Theta_k = \vartheta_k \vartheta_{k-1}$ , then proceed as for the symmetric case by considering the  $\Theta_k \mathcal{Z}_k$  plane, absorbing the signs into  $\mathcal{Z}_k$  defined in Eq. (3.2). An important difference, however, is that  $S_k$  is no longer equal for pulses and antipulses, since

$$S_k = \vartheta_k S. \tag{3.6}$$

Therefore, instead of a single relation like Eq. (3.4), we obtain the two-branched map,

$$\mathcal{Z}_{k+1} = \begin{cases} C_1 - \mathcal{F}(\mathcal{Z}_k) & \text{in } \mathcal{Z} > 0 \\ C_1 + \mathcal{F}(\mathcal{Z}_k) & \text{in } \mathcal{Z} < 0, \end{cases} \tag{3.7}$$

or

$$\mathcal{Z}_{k+1} = \begin{cases} C_1 + \Delta C - \mathcal{F}(\mathcal{Z}_k) & \text{in } \mathcal{Z} > 0 \\ C_1 + \Delta C + \mathcal{F}(\mathcal{Z}_k) & \text{in } \mathcal{Z} < 0, \end{cases} \tag{3.8}$$

with  $C_1 = \beta_1 + S$  and  $\Delta C = -2S$ . ( $\Delta C$  measures the separation of the pulse and antipulse homoclinics at  $\alpha = \varepsilon \alpha_1$ .) Which branch one iterates depends on the polarity of the two pulses under consideration.

Thus, as a consequence of symmetry breaking, the  $\mathcal{Z}_k$  map develops two irreducible branches. This is illustrated in Fig. 5. On transformation to the  $\Theta_k \mathcal{Z}_k$  plane, two of the curves of the equivalent spacing map move into  $\Theta_k \mathcal{Z}_k < 0$  and these correspond to *flip maps* (Fig. 5). The two unchanged branches are *duplication maps* for pulses and anti-

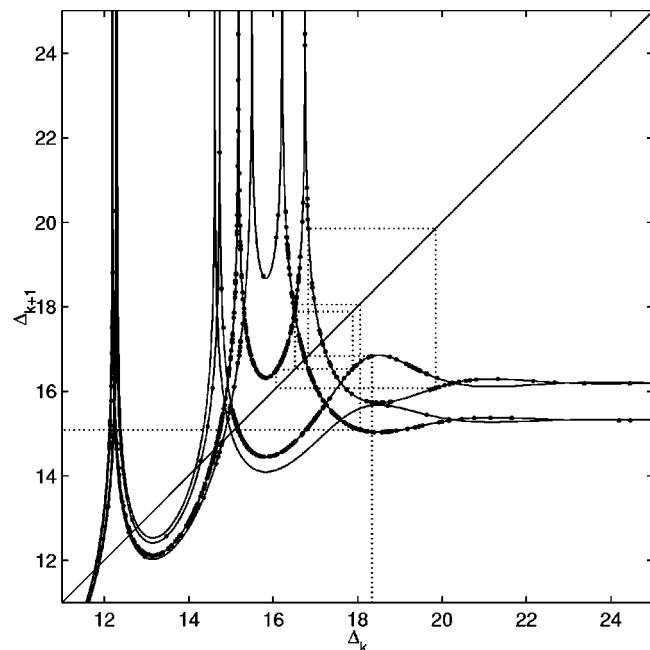


FIG. 4. The spacing map constructed from the solution shown in Fig. 3. The points show the measured spacings, whereas the curves show the four-valued map predicted by perturbation theory [i.e., Eq. (2.13)]. The dotted lines show a sample iteration (the diagonal is also shown).

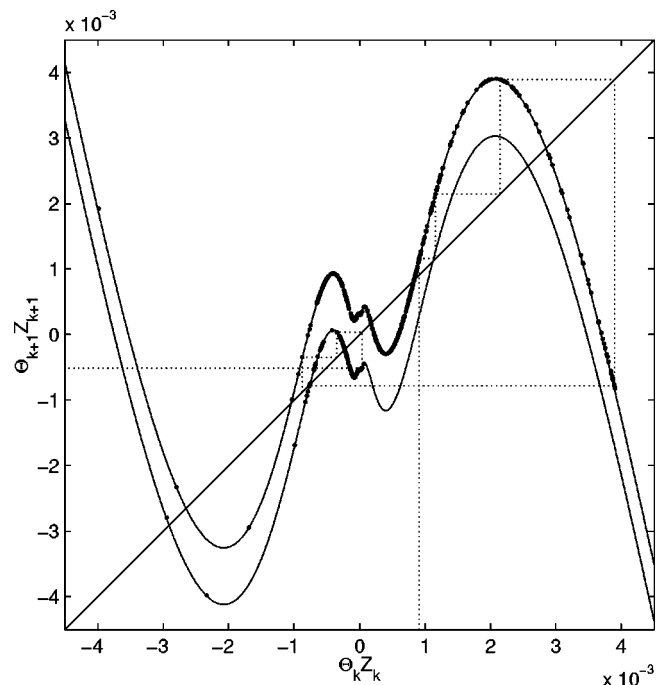


FIG. 5. The  $\Theta_k \mathcal{Z}_k$  map constructed from the solution of Fig. 3. Dots again show measured spacings, converted into values for  $\mathcal{Z}_k$  using Eq. (3.2) and the spacing functions shown in Fig. 2. The solid curves display the double-valued map predicted by asymptotics.

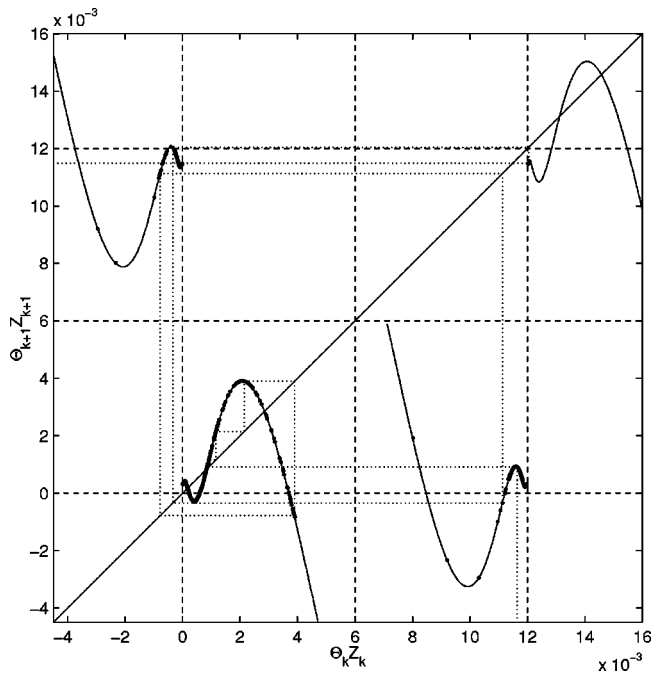


FIG. 6. A single-valued map obtained from the  $Z_k$  map shown in Fig. 5 by breaking the curves into four pieces and placing them into the squares of a checkerboard. Points show measurements and curves indicate the asymptotic theory.

pulses. The remaining twofold multiplicity is removable because the multibranch map can be seen as a one-dimensional map with additional transition rules between each branch. We can construct a checkerboard map<sup>10</sup> from this by breaking apart the four pieces and placing them in a four-square checker board as illustrated in Fig. 6. The location of the pieces within the sixteen boxes follows from the transition rules. It is straightforward to verify that the checkerboard correctly represents the dynamics of the two-branched map.

**C. Strong asymmetry**

As a final example, we consider an asymmetry so extreme that a pulse with a single dominant peak coexists with

a doubly peaked antipulse; Fig. 1(b) displays the relevant homoclinic orbits, and Fig. 2(b) the spacing functions constructed from them. Figure 7 shows a sample solution nearby in parameter space; the corresponding four-valued spacing map appears in Fig. 8. The map (2.13) cannot be simplified any further in this example, but its multiplicity can still be reduced by first reformulating in terms of  $\Theta_k Z_k$  (Fig. 9), where  $Z_k = F_{\downarrow\downarrow}(-\Delta_k)$  and then checker-boarding (Fig. 10). Again, the agreement with the direct numerical results is very good.

**IV. DISCUSSION**

When the solution of differential equations takes the form of a train of pulses that are all nearly alike, it is possible to represent this outcome by an expansion in terms of fundamental structures. In this picture, the pulses in the sequence differ slightly from one another because of their interactions. The approach is different from another expansion that uses (slightly) differing periodic orbits, though there is perhaps some commonality between the two visions. What we have studied here is the extension of the pulse expansions to cases where there are two different kinds of pulses that may enter into the dynamics. This is still a far cry from the case where there is a continuum of pulse types, but we hope that it may be a good beginning.

We have simplified our treatment to finding the rules for successive spacing and kinds of pulses for only a steadily (in some frame) propagating train, but the extension to slowly varying positions is not difficult, as we know from the cited earlier work with one kind of pulse. But there are more generalizations that call for attention.

The restriction to one-dimensional cases with few symmetries leads one to hope that more can be done. What we have looked at here is the extension to the situation where two kinds of objects can interact. The generalization to cases where there are even more kinds of objects, but of a discrete number, looks tractable with additional squares in the checkerboard.

A more difficult issue is that we have studied only cases where the number of pulses in the solution is specified in

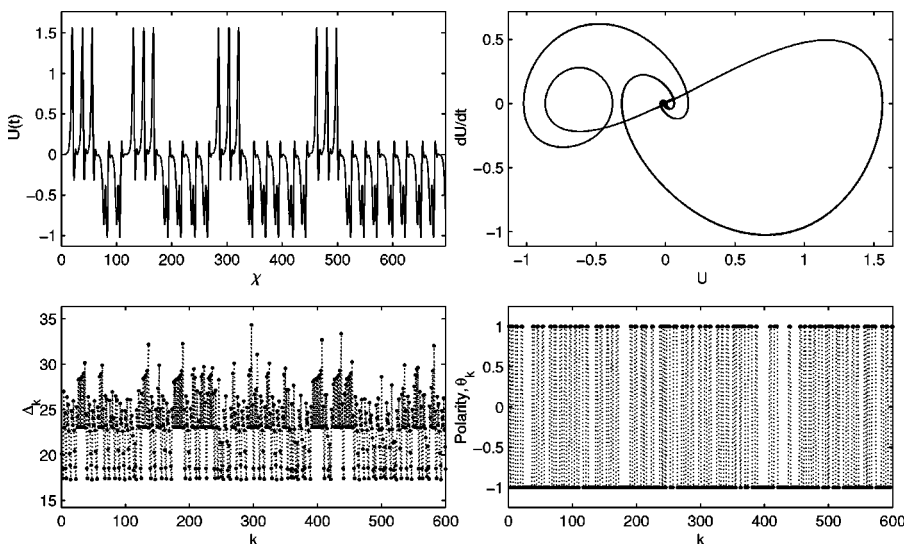


FIG. 7. A numerical solution of Eq. (1.3) with  $\mu=0.81645$ ,  $\alpha=-3.672$ , and  $\beta=0.852806$ . Panels as in Fig. 3.

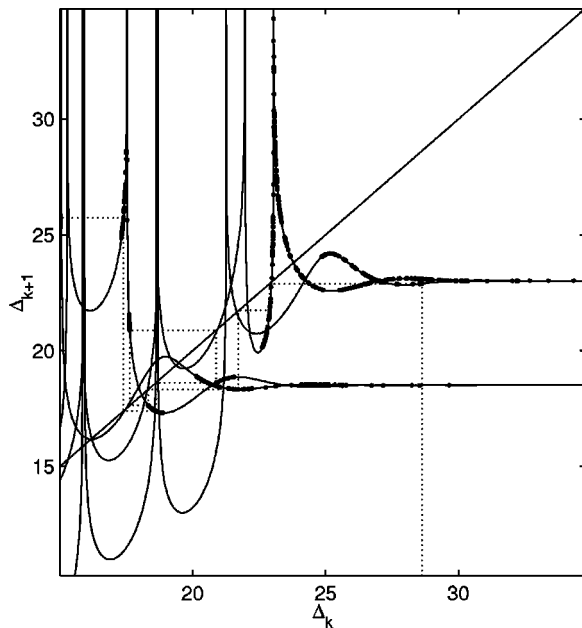


FIG. 8. A similar picture to Fig. 4, but showing the spacing map for the solution of Fig. 7.

advance. Is there a way to allow this number to change in the course of the dynamics? One way to broach this question might be to introduce an analogue of creation and destruction operators for dissipative systems. It is unclear at this time whether such a notion can be made meaningful but a good starting point might be the nearly integrable case that has been studied in some detail.<sup>26</sup>

The inclusion of further group parameters besides position is of interest as well, especially of the amplitude itself when this characteristic is a continuous variable. Also the problem of higher dimensional objects poses some interest-

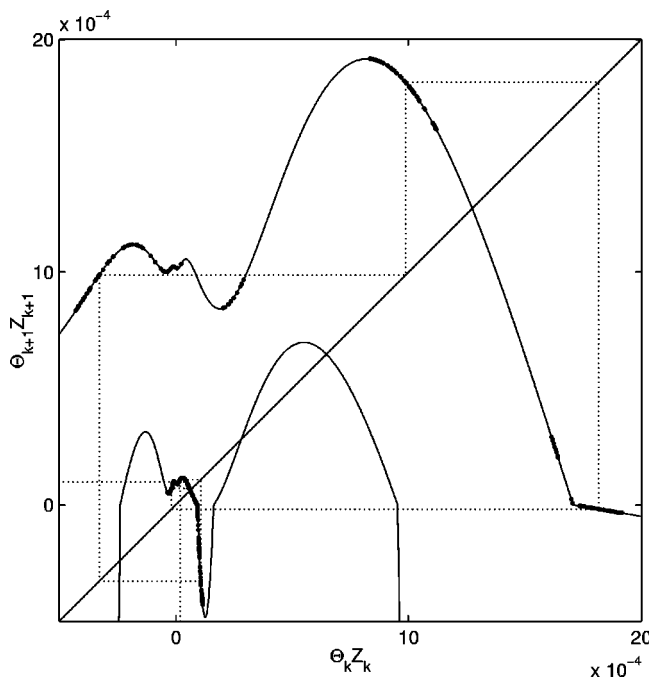


FIG. 9. A similar picture to Fig. 5, but showing the  $Z_k$  map for the solution of Fig. 7.

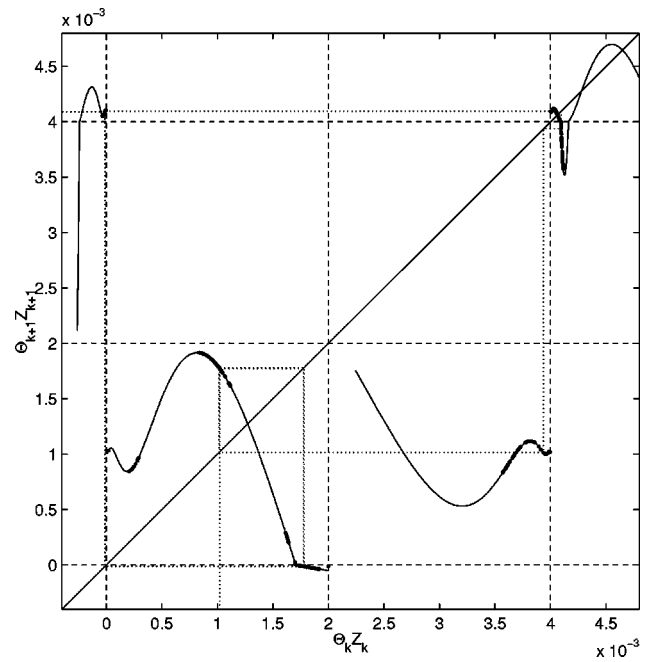


FIG. 10. The single-valued checkerboard map corresponding to Fig. 9.

ing difficulties,<sup>27</sup> particularly in the issue of the interactions of the structures. These are the kinds of questions that the earliest workers grappled with and they are still pretty much open. We hope for more news at the next significant birthdays of our dedicatees.

For now, we must rest our case with the final observation that the asymptotic methods used in this problem appear to provide remarkable accuracy and, on those grounds alone, have proved their worth. One reason that there has been no discernible difference between the numerical and the asymptotic solutions is probably that the asymptotics does not seem to lead to small pulse spacings, though these are allowed by the procedure. No doubt it would be best in asymptotic studies to rule out cases with small pulse separations, for these are outside the domain of validity of the pulse expansions (this was our basic premise in ignoring the ambiguities at small spacing when inverting the space function  $F$ ). However, as yet, we have seen no problems arising from this aspect of the work.

- <sup>1</sup> A. Einstein, L. Infeld, and B. Hoffman, "The gravitational equations and the problem of motion," *Ann. Math.* **39**, 65–110 (1938).
- <sup>2</sup> P. Cvitanovic, *Field Theory* (Nordita Lecture Notes, Copenhagen, 1983).
- <sup>3</sup> J.R. Keener and D.W. McLaughlin, "Solitons under perturbation," *Phys. Rev. A* **16**, 777–785 (1977).
- <sup>4</sup> K.A. Gorshkov and L.A. Ostrovsky, "Interactions of solitons in nonintegrable systems: Direct perturbation method and applications," *Physica D* **3**, 428–438 (1981).
- <sup>5</sup> K. Kawasaki and T. Ohta, "Kink dynamics in one-dimensional nonlinear systems," *Physica A* **116**, 573–593 (1982).
- <sup>6</sup> P. Coullet, C. Elphick, and D. Repaux, "Nature of spatial chaos," *Phys. Rev. Lett.* **58**, 431–438 (1987).
- <sup>7</sup> C. Elphick, E. Meron, and E.A. Spiegel, "Patterns of propagating pulses," *SIAM (Soc. Ind. Appl. Math.) J. Appl. Math.* **50**, 490–503 (1990).
- <sup>8</sup> N.J. Balmforth, "Coherent structures and homoclinic orbits," *Annu. Rev. Fluid Mech.* **27**, 335–355 (1995).
- <sup>9</sup> N.J. Balmforth, G.R. Ierley, and R. Worthing, "Pulse dynamics in an unstable medium," *SIAM (Soc. Ind. Appl. Math.) J. Appl. Math.* **56**, 205–225 (1997).

- <sup>10</sup>N.J. Balmforth, E.A. Spiegel, and C. Tresser, "Checkerboard maps," *Chaos* **5**, 216–226 (1995).
- <sup>11</sup>H.-C. Chang, E.A. Demekhin, and D.I. Kopelevich, "Laminarizing effects of dispersion in an active-dissipative nonlinear medium," *Physica D* **63**, 299–320 (1993).
- <sup>12</sup>N.J. Balmforth, G.R. Ierley, and E.A. Spiegel, "Chaotic pulse trains," *SIAM (Soc. Ind. Appl. Math.) J. Appl. Math.* **54**, 1291–1234 (1994).
- <sup>13</sup>P. Coullet and C. Elphick, "Topological defect dynamics and Melnikov's theory," *Phys. Lett. A* **121**, 233–236 (1987).
- <sup>14</sup>P. Glendinning, "Bifurcations near homoclinic orbits with symmetry," *Phys. Lett. A* **103**, 163–166 (1984).
- <sup>15</sup>D.J. Benney, "Long waves on liquid films," *J. Math. Phys. (Cambridge, Mass.)* **45**, 150–155 (1966).
- <sup>16</sup>G.M. Homsy, "Model equations for wavy viscous film flow," *Lect. Appl. Math.* **15**, 191–194 (1974).
- <sup>17</sup>B.S. Tilley, S.H. Davis, and S.G. Bankoff, "Nonlinear long-wave stability of superposed fluids in an inclined channel," *J. Fluid Mech.* **277**, 55–83 (1994).
- <sup>18</sup>D.W. Moore and E.A. Spiegel, "A thermally excited nonlinear oscillator," *Astrophys. J.* **143**, 871 (1966).
- <sup>19</sup>A. Arneodo, P.H. Coullet, and E.A. Spiegel, "Dynamics of triple convection," *Geophys. Astrophys. Fluid Dyn.* **31**, 1–48 (1985).
- <sup>20</sup>A. Arneodo, P.H. Coullet, E.A. Spiegel, and C. Tresser, "Asymptotic chaos," *Physica D* **14**, 327–347 (1985).
- <sup>21</sup>P. Glendinning and C. Sparrow, "Local and global behaviour near homoclinic orbits," *J. Stat. Phys.* **35**, 645–696 (1984).
- <sup>22</sup>V. Degiorgio, R. Piazza, M. Corti, and C. Minero, "Critical properties of nonionic micellar solutions," *J. Chem. Phys.* **82**, 1025 (1985).
- <sup>23</sup>C. Elphick, E. Meron, J. Rinzel, and E.A. Spiegel, "Impulse patterning and relaxational propagation in excitable media," *J. Theor. Biol.* **146**, 249–268 (1990).
- <sup>24</sup>K.B. Glasner and T.P. Witelski, "Coarsening dynamics of dewetting films," *Phys. Rev. E* **67**, 016302 (2003).
- <sup>25</sup>S. Toh and T. Kawahara, "On the stability of soliton-like pulses in a nonlinear dispersive system with instability and dissipation," *J. Phys. Soc. Jpn.* **54**, 1257–1267 (1985).
- <sup>26</sup>D.J. Kaup and A.C. Newell, "Solitons as particles, oscillators, and in slowly changing media: A singular perturbation theory," *Proc. R. Soc. London, Ser. A* **361**, 413–446 (1978).
- <sup>27</sup>M.I. Rabinovich, A.B. Ezersky, and P.D. Weidman, *The Dynamics of Patterns* (World Scientific, Singapore, 2000), Chap. 8.